Temperature and Flow Rate of NH_3 Effects on Nitrogen Content and Doping Environments of Carbon Nanotubes Grown by Injection CVD Method

Jiwen Liu, Scott Webster, and David L. Carroll*

The Center for Nanotechnology and Molecular Materials, Department of Physics, Wake Forest University, Winston-Salem, North Carolina 27109

Received: January 7, 2005; In Final Form: April 19, 2005

Large-scale and vertically aligned nitrogen-doped carbon nanotubes were synthesized by pyrolysis of pyridine with ferrocene as the catalysts under either pure NH_3 or a mixture of NH_3 and argon atmosphere using injection chemical vapor deposition method. Nitrogen content ranges from 4.8 at. % to 8.8 at. % and changes as a function of growth temperature and the flow rate of NH_3. NH_3 not only increases the nitrogen content of carbon nanotubes but also increases the proportion of pyridine-like N doping in the carbon nanotubes. It suggests that nitrogen concentration and nitrogen doping environments of carbon nanotubes could be controlled by changing the growth temperature or flow rate of NH_3.

1. Introduction

The theoretical prediction that materials conforming to a C_3N_4 stoichiometry could likely be hardest known[1] and the potential for altering the electronic properties of carbon nanotubes[2−3] have triggered several attempts[4−13] to incorporate nitrogen into carbon nanotubes. At present, most studies show that the highest N content in CN_x nanotubes lies in the range from 2 at. % to 9 at. %, which is much lower than that in C_3N_4. For example, Sen et al.[12] have prepared nitrogen-doped carobn nanotubes with nitrogen concentration from 3 at. % to 9 at. % by pyrolyzing pyridine over Co catalyst. Aligned CN_x nanotubes with nitrogen concentration of 2 at. % have been prepared by pyrolyzing triazine over a laser-patterned Co substrate.[4] CN_x ($x = 0.07$) nanofibers have also been prepared by pyrolysis of nitrogen-rich organic precursors.[14] Han et al.[15] concluded that pyrolysis in the atmosphere of NH_3 provides an efficient route to higher nitrogen content carbon nanotubes than can be achieved using nitrogen gas or nitrogen-containing solid precursors such as melamine, after comparing the results obtained by pyrolyzing ferrocene/melamine/Ar, ferrocene/C_{60}/NH_3, and ferrocene/C_{60}/N_2. Recently, Lee et al. have also synthesized CN_x nanotubes (2.8−6.8 at. % N) using $C_2H_2-NH_3-Fe(CO)_5$ system.[16] They further confirm NH_3 is an effective nitrogen source for doping of carbon nanotubes. Very recently, Tang[17] and Glerrup[18] et al. demonstrated that a much higher concentration range from ∼10% to ∼20% could be synthesized when acetonitrile or DMF was used as precursors because nearly all of the nitrogen could be used in the reaction and doped into the carbon lattice. Lee et al.[16] reported that the nitrogen concentration increases with the growth temperature increasing when NH_3 was used as nitrogen source, and Tang[17] et al. reported that the nitrogen concentration decreases with the growth temperature increasing when DMF was used as the precursor. However, there have not been many systematic studies on the synthesis of large quantities of nitrogen carbon nanotubes with high nitrogen content and equally little work on how the growth conditions affect the nitrogen-doping concentration and doping environment within the carbon nanotubes.

Our earlier works[19,20] have shown that pyridine is a good precursor for large-scale, highly aligned nitrogen-doped carbon nanotube growth. However, the nitrogen concentration falls only between 1 at. % and 2 at. %, although the nitrogen has been shown to substitute into the carbon lattice as both pyridinic and graphitic forms. In this paper, we report an efficient way to greatly increase the nitrogen concentration level of carbon nanotubes by using NH_3 instead of H_2 as in our earlier work. X-ray photoelectron spectroscopy (XPS) shows the nitrogen concentration of the carbon nanotubes can be increased to over 8 at. %.

2. Experimental Section

The experimental setup is similar to that for pure carbon nanotube growth[21] and is also described elsewhere.[20] Briefly speaking, the setup consists of two furnaces, one is a preheater and the other is a growth reactor. During growth, 2.7 wt. % of ferrocene was dissolved in pyridine and was fed into the preheater (200 °C) by an injection pump with the feed rate of 5 mL/h. The volatilized reaction gas was swept into the reactor by a flow of NH_3 or a mixture of NH_3 and argon with a total flow rate of 320 sccm. When pure NH_3 was used, the growth temperature ranged from 750 °C to 1000 °C. When at constant growth temperature of 750 °C, the flow rate of NH_3 ranged from 40 sccm to 280 sccm while the total flow rate was kept constant, 320 sccm. After a 1-h growth, the NH_3 was switched to pure argon with the same flow rate and the furnace was allowed to cool to room temperature.

Scanning electron microscopy (SEM) (Hitachi S-4700, 20 KV) and transmission electron microscopy (TEM) (Hitachi HD-2000, 200 KV and FEI Tecnai F30, 300 KV) were used to check the quality, layer structure, and overall morphology of the nanotubes. X-ray photoelectron spectroscopy (XPS) (Kratos AXIS 165) was used to examine the stoichiometry of the carbon and nitrogen atoms and the intensity of the two types of carbon−nitrogen bonding. Raman spectroscopy was performed using Horiba Jobin Yvon's high-resolution LabRam with a 50× collection objective with an excitation source of 632.8 nm HeNe at constant power and integration times.

* Corresponding author. E-mail: carroldl@wfu.edu.

10.1021/jp050123b CCC: $30.25
Published on Web 07/28/2005

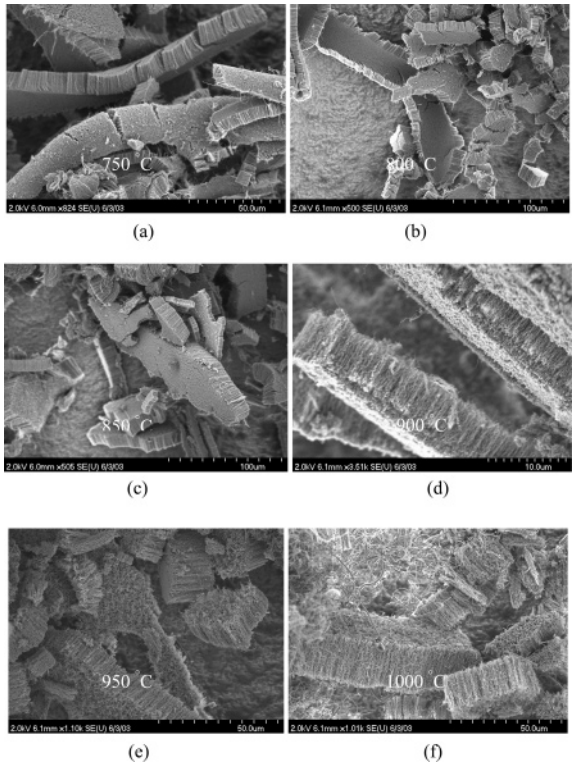

Figure 1. (a−f) SEM images of carbon nanotubes grown at different temperatures under pure NH_3. The temperature is increasing for images a−f.

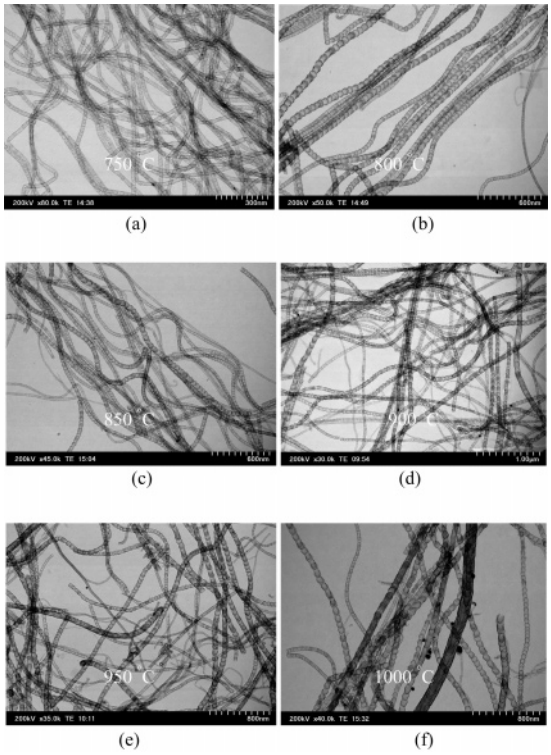

Figure 2. (a−f) TEM images of carbon nanotubes grown at different temperatures in the presence of pure NH_3. As the images go from a−f, the temperature increases.

3. Results and Discussions

I. Temperature Effect. A dense film was observed to deposit inside the quartz reactor over a wide temperature range from 750 °C to 1000 °C, and the sample can be peeled off the quartz tube. Figure 1 shows SEM micrographs of the N-doped carbon nanotubes grown at different temperatures under pure NH_3 while other growth conditions are the same. At lower growth temperatures, for example, at 750 °C (Figure 1a), the tubes form a dense film and are very well aligned. As the growth temperature increases, a carbon nanotube film can still be obtained even at 1000 °C (Figure 1f). However, the film is less dense than that grown at lower temperatures and some big fibers over 100 nm are observed at 1000 °C. As the growth temperature increases, more agglomeration occurs at higher growth temperature, which results in a larger sized catalyst with low density. The thickness of the film in the presence of pure NH_3 is lower than that in the presence of H_2. For example, the thickness of nanotubes grown at 750 °C in the presence of pure H_2 is about 100 μm after 1 h growth as indicated in our earlier work[20] while the thickness of the carbon nanotube film grown at the same temperature in the presence of pure NH_3 is only around 20 μm after 1 h growth. It suggests that NH_3 plays an important role in the growth rate and decreases the growth rate of carbon nanotubes. The possible reason for this is that the nitrogen from the decomposition of NH_3 is adsorbed on the surface of the iron particles and restrains the surface diffusion of carbon, which limits the growth rate of carbon nanotubes[16] and thus leads to a decrease in the growth rate of the nanotubes.

Figure 2 a−f shows TEM images of carbon nanotubes grown at different temperatures from 750 °C to 1000 °C in the presence of pure NH_3. All of the carbon nanotubes grown at different temperatures are very clean and free of amorphous carbon. At lower growth temperatures, the carbon nanotubes have a more uniform diameter than those grown at higher growth temperatures, and the average diameter at lower growth temperature is less than that at higher growth temperature. For example, the average diameter of the carbon nanotubes grown at 750 °C is about 40 nm, while the average diameter of the carbon nanotubes grown at 950 °C is about 65 nm. However, the average diameter for all growth temperatures is larger than that from pyrolysis of pyridine in the presence of pure H_2 at the same growth temperatures. For example, the average diameter of the carbon nanotubes grown from pyridine in the presence of H_2 at 750 °C is about 25 nm, which is less than that of carbon nanotubes grown in the presence of NH_3 at the same growth temperature. This may be explained by improved kinetics of the Fe particle coalescence because of decomposition of NH_3 on the surface of the Fe particles compared to that in the presence of pure H_2. In other words, decomposition of NH_3 may enhance the agglomeration effect causing more Fe nanoparticles to melt together to become bigger Fe particles and therefore resulting in larger diameter carbon nanotubes. Consistent with that observed from SEM (Figure 1f), large fibers with diameters over 100 nm are found from TEM observation for the carbon nanotubes grown at 1000 °C as shown in Figure 2f. Another important feature for the carbon nanotubes grown in the NH_3 at all different growth temperatures is that the structure of the tubes is bamboolike because of to nitrogen doping.

To look for the nitrogen content in the growth materials, XPS was carried out on the tubes grown at different temperatures. All XPS spectra from the tubes show that the nanotubes consist of carbon accompanied by traces of nitrogen. The C 1s signal is at ~285 eV (Figure 3 a) and the N 1s signal is about 400 eV as indicated in Figure 3b. The N 1s signal is much stronger than that grown without the presence of NH_3, and this suggests a higher nitrogen concentration presented in these carbon nanotubes. By taking the ratio of the integrated peak areas under the C 1s and N 1s signal (without spectral decomposition) and dividing them by the respective photoionization cross section

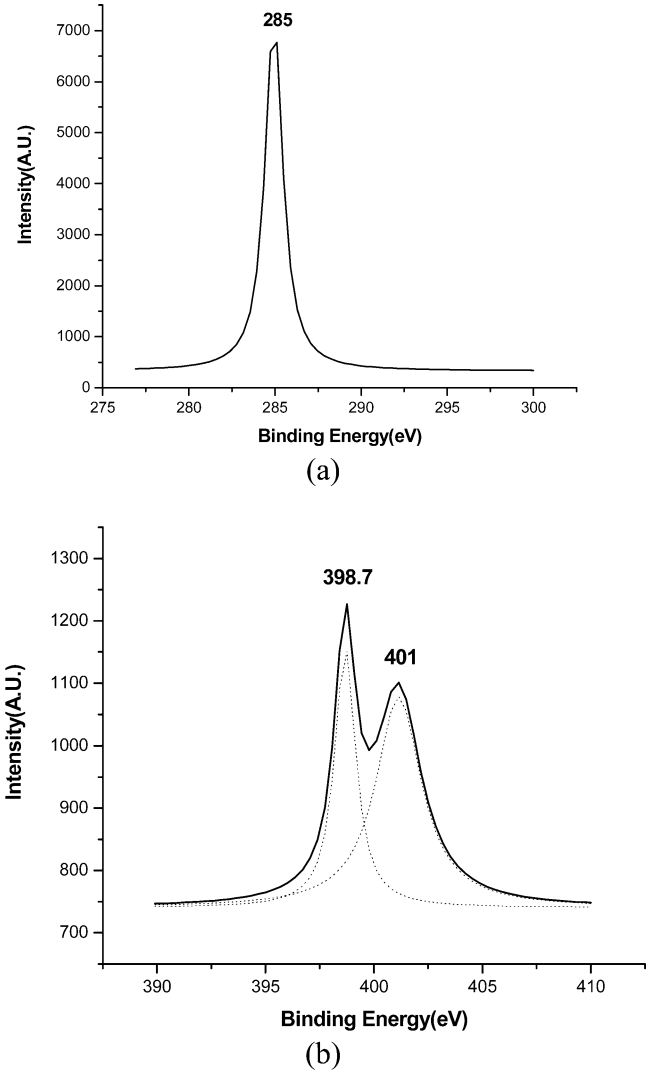

Figure 3. XPS spectra of C 1s element (a) and N 1s signal (b) for the nitrogen-doped carbon nanotubes grown at 850 °C in the presence of NH_3.

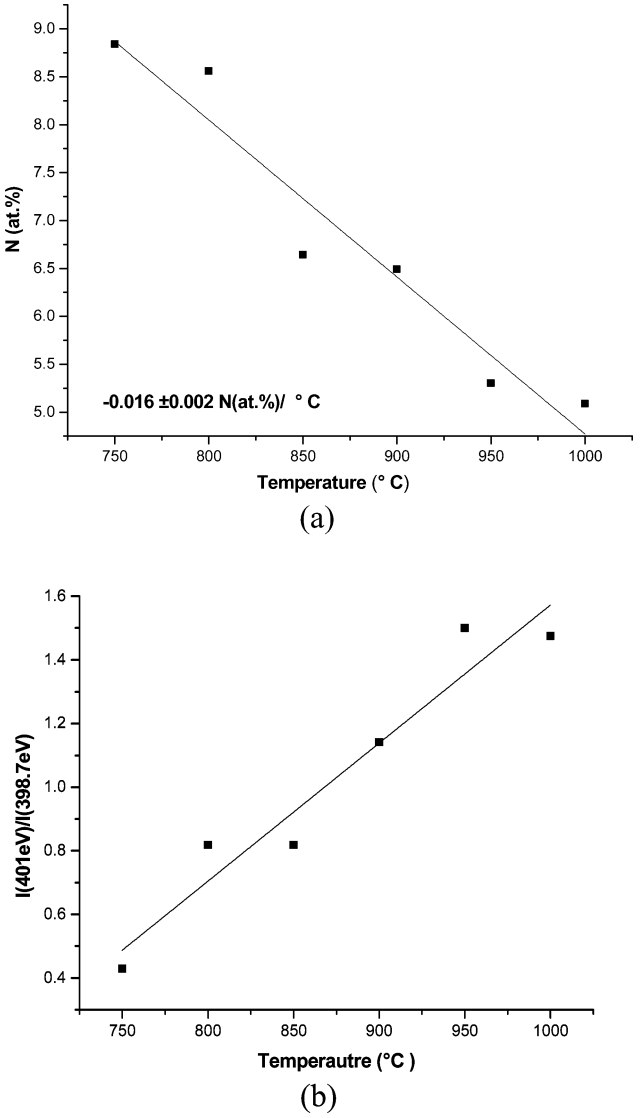

Figure 4. (a) The nitrogen concentration decreases as the growth temperatures increase in the presence of pure NH_3. (b) The intensity ratio of 401 eV/398.7 eV changes with the growth temperature in the presence of pure NH_3.

for the 1s level,[22] the nitrogen concentration of carbon nanotubes grown in the temperature range from 750 °C to 1000 °C can be estimated to fall between 4.8% and 8.8%, and it decreases at the rate of 0.016% N/°C as the growth temperature increases (Figure 4 a). Since the C−C bonding energy (370 kJ/mol) is higher that the C−N bonding energy (305 kJ/mol), it is expected that the C−C bonding is more favorable than C−N bonding at high growth temperatures.[23] Another possible reason is that stable N_2 molecules form and is liberated as the growth temperature increases.[7]

However, it is clear that the nitrogen concentration of carbon nanotubes is much higher than when H_2 is used, and the highest nitrogen concentration can be reached as high as 8.8 at. % at 750 °C. Further, the carbon nanotubes in our experiments are free of any other kinds of carbon forms and are aligned very well, especially with high yield compared to the nitrogen carbon nanotubes grown by any other methods.

There are several ways in which N can be incorporated in the carbon nanotube lattice.[3,24−25] However, there are only two ways observed in our studies. One is pyridine-like and the other is graphite-like as reported in our earlier studies and by other groups[7,9,26] whose bonding energies are 398.7 eV and 401 eV, respectively. Also, we know that the intensity ratio of *I*(401 eV)/*I*(398.7 eV) increases with increasing growth temperature. By using pure NH_3 instead of H_2, the N 1s signal for the carbon nanotubes grown at all temperatures from 750 °C to 1000 °C also clearly shows two distinct features at 398.7 eV and 401 eV (Figure 3b) like that in the presence of pure H_2, which corresponds to pyridine-like and graphite-like, respectively. For example, Figure 4 shows the N 1s signal for the carbon nanotubes synthesized at 900 °C. The two features are resolved here. The pyridine-like structure still has an apparent feature at 1000 °C in NH_3 growth, but when the tubes are grown with H_2, the feature gradually disappears as growth temperature increases and is almost undetectable at 900 °C.[20] Further, the intensity ratio of *I*(401 eV)/*I*(398.7 eV) changes with the growth temperature under NH_3 atmosphere and is shown in Figure 4b.

The intensity ratio of 401 eV/398.7 eV in the presence of NH_3 is much lower compared to the intensity ratio in the presence of pure H_2 as shown in our earlier work.[20] For example, the ratio of 401 eV/398.7 eV at 750 °C in the presence of H_2 is 2.7, while the ratio is only 0.43 in the presence of NH_3. Apparently, a larger proportion of pyridine-like N is presented in the carbon nanotubes grown under NH_3 atmosphere. Second, as the growth temperature increases from 750 °C to 1000 °C, the ratio of 401 eV/398.7 eV shows an increasing trend; this

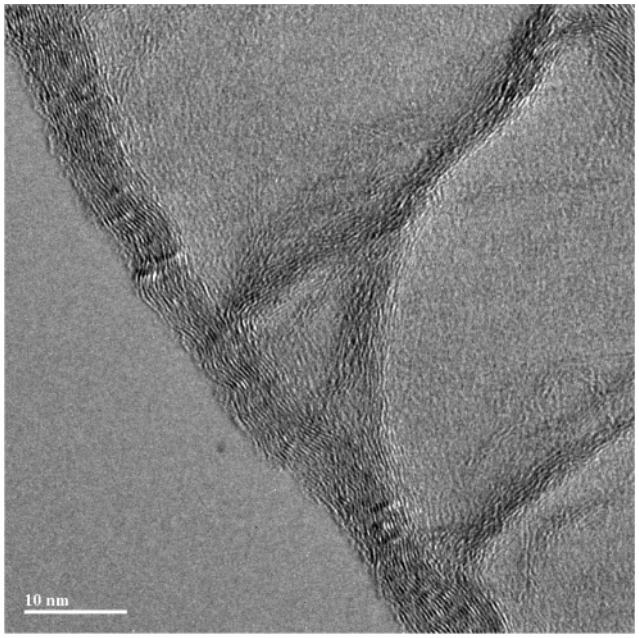

(a)

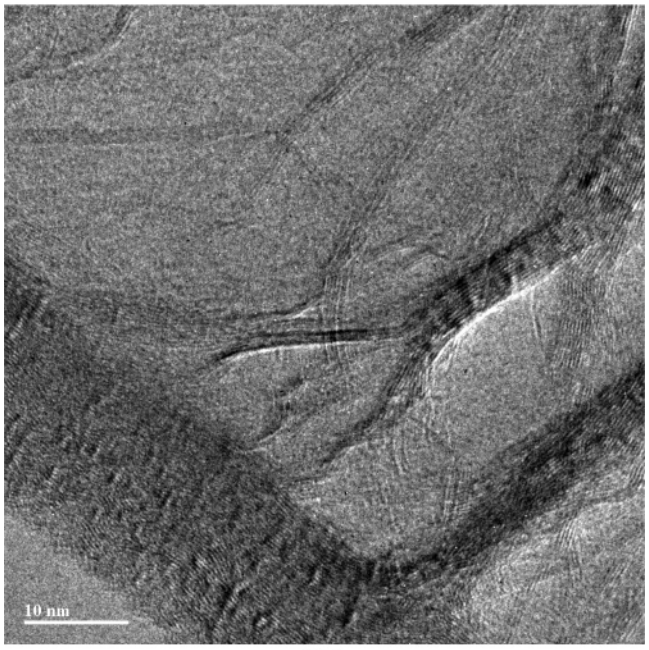

(b)

Figure 5. (a) HRTEM image for a 6.6% nitrogen-doped carbon nanotube grown at 850 °C under pure NH_3. (b) HRTEN iamge for a 4.8% nitrogen-doped carbon nanotube grown at 1000 °C under pure NH_3.

means the proportion of pyridine-like N decreases as the growth temperature increases. From Figure 4a, we know that the nitrogen concentration decreases with increasing of the growth temperature. So, in other words, the proportion of pyridine-like N decreases when the nitrogen concentration decreases. This result is consistent with previous reports for nitrogen-doped carbon nanofibers[7] and carbon nanotubes[9] when melamine is used as a precursor. So, these results suggest that NH_3 not only increases the nitrogen concentration of the carbon nanotubes but also increases the proportion of pyridine-like N compared with the case of H_2 at the same growth temperature, and the

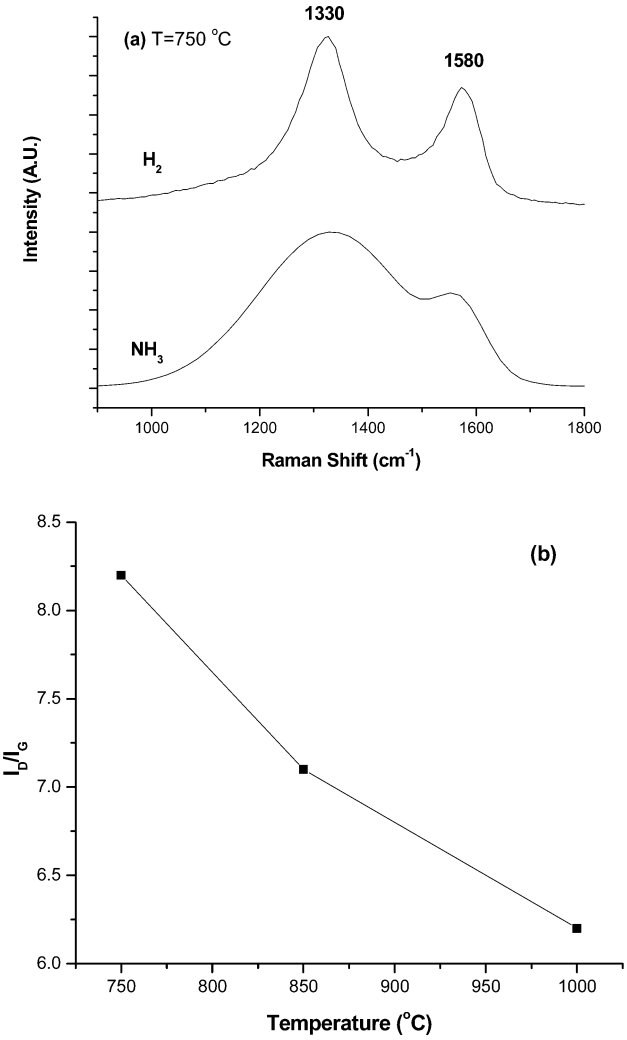

Figure 6. (a) Raman spectrum for 1.5% nitrogen-doped carbon nanotubes and 8.8% nitrogen-doped carbon nanotubes grown at 750 °C under pure H_2 and pure HN_3, respectively. (b) Plot of the I_D/I_G value vs the growth temperature under pure NH_3.

proportion of pyridine-like N increases as the overall nitrogen concentration increases.

Figure 5a shows an HRTEM image for a 6.6% nitrogen-doped carbon nanotube grown at 850 °C under 320 sccm NH_3 flow. The surface of the wall is rough and the graphitic sheets of the wall are waved over a long range, showing the lower degree of crystalline perfection than that of a 4.8% nitrogen-doped carbon nanotube grown at 1000 °C under NH_3 (Figure 5b). The compartment layers within the two tubes show interlinked morphology. However, the 6.6% nitrogen-doped carbon nanotube shows lower low crystalline perfection that that of 4.8% nitrogen-doped tube. We believe the nitrogen doping in the pyridine-like N sites is responsible for both the wall roughness and interlinked morphologies.[8] As the number of pyridine-like sites increases within tubes, the roughness of both the tube wall and the compartment layers increases.

Raman spectra were taken from the tubes grown at 750, 850, and 1000 °C under pure NH_3, and the nitrogen concentration of the tubes are 8.8, 6.6, and 4.8%, respectively. Figure 6a shows Raman spectra taken from the tubes grown under pure NH_3 at 750 °C. Spectrum taken from the tubes with 1.5% N grown at 750 °C under pure H_2 is also displayed for comparison. All spectra show mainly two bands at $\sim$1330 cm^{-1} (D-band) and $\sim$1580 cm^{-1} (G-band). The D-band indicates the defective

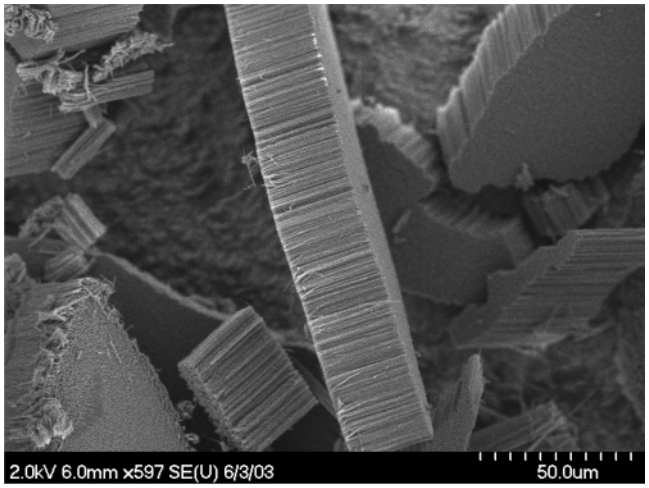

(a)

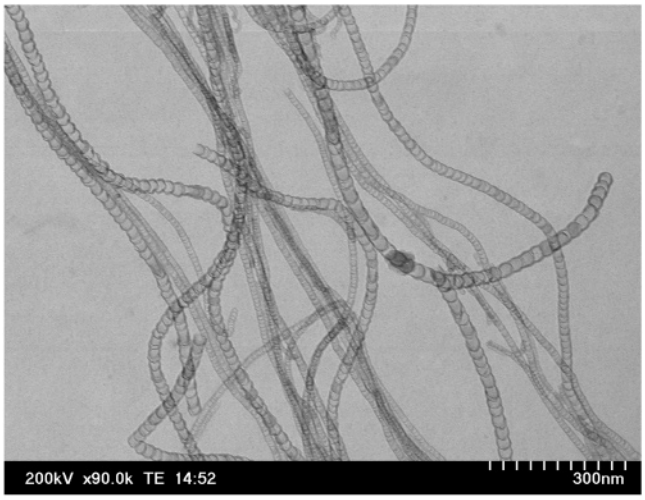

(b)

Figure 7. (a) SEM picture of nanotube mats grown with 280 sccm NH_3 flow at 750 °C. (b) TEM picture of nanotube mats grown with 280 sccm NH_3 flow at 750 °C.

structure of graphite sheets.[27] It is clearly seen that the D-band becomes much broader as nitrogen concentration increases. At 750 °C, the I_D/I_G value for tubes grown with pure H_2 is 2.1. However, this value increases to 8.2 when using NH_3 instead of H_2. This suggests that many more defects are mostly pyridine-like sites and are introduced because of NH_3 use. Further, this confirms that NH_3 can greatly enhance the nitrogen doping, especially pyridine-like sites within carbon nanotubes. Figure 6b shows a plot of the I_D/I_G value versus the growth temperature under pure NH_3. As the growth temperature increases from 750 °C to 1000 °C, the I_D/I_G decreases from 8.2 to 6.2. There are two factors which effect the I_D/I_G decrease. One is that the crystalline perfection increases with the increasing growth temperature and the other results from nitrogen concentration from 8.8% to 4.8%, mostly pyridine-like sites decreases. This suggests that the increasing of pyridinic sites within the carbon nanotubes increases the I_D/I_G ratio.

II. NH_3 Flow Rate Effect. We chose 750 °C as the constant growth temperature and NH_3/Ar mixture with a total flow rate of 320 sccm. The flow rate of NH_3 was selected as 40, 120, 200, and 280 sccm, while the other growth conditions are the same as that used for growth at different temperatures. Aligned carbon nanotube films can still be synthesized in this range of

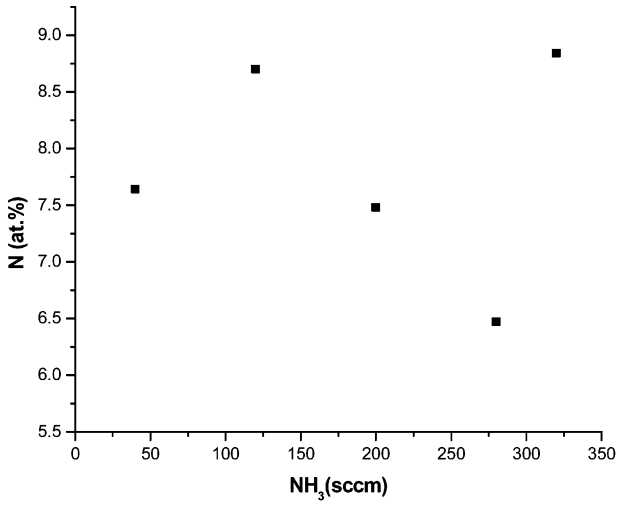

(a)

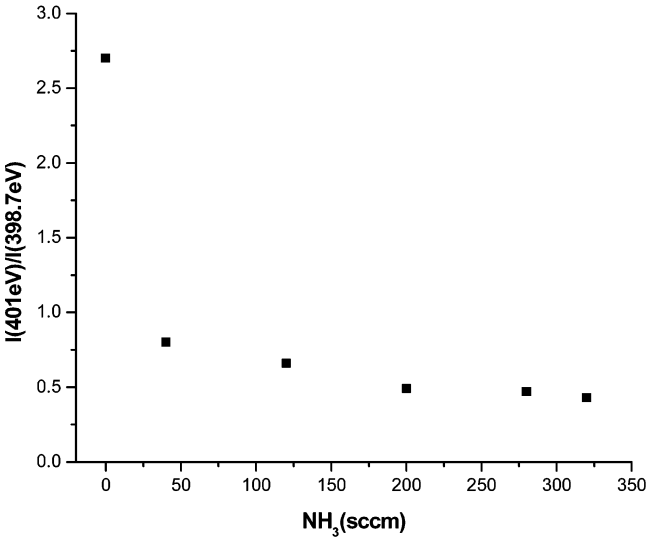

(b)

Figure 8. (a) The nitrogen concentration changes with the NH_3 flow rate at 750 °C. (b) The intensity ratio of 401 eV/398.7 eV changes with the NH_3 flow rate at 750 °C.

NH_3 flow rates as shown in SEM observations. For example, Figure 7a shows carbon nanotube mats grown with 280 sccm NH_3 flow. It is observed that the thickness of the films grown at different NH_3 flow rate range from 40 to 280 sccm falls between ~25 and 50 μm and that there is no obvious relationship between the NH_3 flow rate and the thickness of the carbon nanotube film. The tubes have the same bamboo structures as that grown under pure NH_3 flow as shown in Figure 7b for the tubes grown at 750 °C with 280 sccm NH_3 flow. The diameter ranges from 25 nm to 55 nm and the average diameter is ~40 nm, which is almost the same as the tubes grown at 750 °C under pure NH_3. This suggests that the diameter is determined by the growth temperature.

All XPS spectra show that the carbon nanotubes grown with different NH_3 flow rate from 40 to 280 sccm also consist of carbon accompanied by traces of nitrogen. The C 1s signal is at ~285 eV and the N 1s signal is about 400 eV. Nitrogen concentration of these samples was calculated by taking the ratio of the integrated peak areas under the C 1s and N 1s signal (without spectral decomposition) and dividing them by the respective photoionization cross section for the 1s level.[22] At

40 sccm NH_3 flow, the nitrogen concentration is ~7.6 at. % and increases to 8.7 at. % when the NH_3 flow is 120 sccm. Again, NH_3 can greatly increase the nitrogen concentration of carbon nanotubes. However, as the NH_3 flow rate continues increasing till 280 sccm, the nitrogen content decreases to ~6.4 at. %. Figure 8a is the plot of nitrogen content as a function of NH_3 flow rate. From the data shown here from 40 to 280 sccm NH_3 flow, while the total flow rate is 320 sccm, we found that the maximum N content in the present nitrogen-doped carbon nanotubes is about 8.7 at. %. This result is consistent with the result obtained by Lee et al.[28] Also, the nitrogen content increases again to 8.8 at. % when using pure NH_3 with flow rate of 320 sccm. However, it is not clear how to explain the nitrogen content decrease at the higher flow rate of NH_3 and why the nitrogen content comes back to the maximum when pure NH_3 is used.

By using a mixture of NH_3 and Ar, the N 1s signal for the carbon nanotubes grown at all different NH_3 flow rates from 40 to 280 also clearly and only shows two distinct features at ~398.7 eV and ~401 eV, which correspond to pyridine-like and graphite-like structures, respectively. We already know that the ratio of 401 eV over 398.7 eV of the nitrogen-doped carbon nanotubes is ~2.7 when using pure H_2 at 750 °C.[18] Figure 8b shows the intensity ratio of 401 eV over 398.7 eV as a function of the NH_3 flow rate. When 40 sccm NH_3 is used, this ratio dcreases dramatically to 0.8. This suggests that the more pyridine-like structures presented in the carbon lattice is due to the presence of NH_3. As the NH_3 flow rate increases to 320 sccm, this ratio continues decreasing slightly to 0.43. So, in the whole NH_3 flow rate range from 0 to 320 sccm, the intensity ratio of 401 eV over 398.7 eV decreases with increasing the flow rate. This means the proportion of pyridine-like structures in the carbon lattice increases with NH_3 flow rate increasing, and this further confirms that NH_3 can contribute more pyridine-like structure doping into the carbon nanotube lattice.

4. Conclusions

Nitrogen-doped carbon nanotubes can be synthesized by pyrolysis of pyridine with ferrocene as the catalyst under pure NH_3 atmosphere or a mixture of NH_3 and Ar. The nitrogen concentration is greatly enhanced by introducing NH_3 in comparison with that using H_2 as the carrier gas. The highest nitrogen concentration of carbon nanotubes can get to 8.8 at. % at 750 °C and decreases when the growth temperature increases under pure NH_3 atmosphere, while there exists a maximum nitrogen content around 120 sccm NH_3 when using a mixture of NH_3 and Ar at 750 °C. NH_3 not only increases the nitrogen concentration of the carbon nanotubes but also increases the proportion of pyridine-like N compared with the case of H_2 at the same growth temperature, and the proportion of pyridine-like N increases as the overall nitrogen concentration increases. The proportion of pyridine-like structure decreases with increasing growth temperature under pure NH_3 atmosphere, while the pyridine structure increases with increasing the flow rate of NH_3. From these results, we believe that it is possible to control nitrogen concentration of carbon nanotubes and nitrogen-bonding types by changing growth conditions, such as growth temperature, NH_3 flow rate, and so forth, and this is important to the further application of doped carbon nanotubes.

Acknowledgment. This work was supported at Wake Forest University by the Air Force Office of Sponsored Research (AFOSR) under grant no. FA9550-04-1-0161. The authors also thank Mr. Zia Rahman in the Materials Characterization Facility (AMPAC) at the University of Central Florida for his assistance with the FEI Tecnai F30 TEM.

References and Notes

(1) Liu, A. Y.; Cohen, M. L. *Science* **1989**, *245*, 841.
(2) Teter, D. M.; Hemley, R. J. *Science* **1996**, *271*, 53.
(3) Miyamoto, Y.; Cohen, M. L.; Louie, S. G. *Solid State Commun.* **1997**, *102*, 605.
(4) Terrones, M.; Grobert, N.; Olivares, J.; Zhang, J. P.; Terrones, H.; Kordatos, K.; Hsu, W. K.; Hare, J. P.; Kroto, H. W.; Prassides, K.; Cheetham, A. K.; Townsend, P. D.; Walton, D. R. M. *Nature* **1997**, *388*, 52.
(5) Terrones, M.; Kamalakaran, R.; Seeger, T.; Rühle, M. *Chem. Commun.* **2000**, *23*, 2335.
(6) Suenaga, K.; Yudasaka, M.; Colliex, C.; Iijima, S. *Chem. Phys. Lett.* **2000**, *316*, 365.
(7) Terrones, M.; Redlich, P.; Grobert, N.; Trasobares, S.; Hsu, W. K.; Terrones, H.; Zhu, Y. Q.; Hare, J. P.; Reeves, C. L.; Cheertham, A. K.; Rühle, M.; Kroto, H. W.; Walton, D. R. M. *Adv. Mater.* **1999**, *11*, 655.
(8) Terrones, M.; Terrones, H.; Grobert, N.; Trasobares, S.; Hsu, W. K.; Zhu, Y. Q.; Hare, J. P.; Kroto, H. W.; Walton, D. R. M.; Redlich, P. K.; Rühle, M.; Zhang, J. P.; Cheertham, A. K. *Appl. Phys. Lett.* **1999**, *75*, 3932.
(9) Terrones, M.; Ajayan, P. M.; Banhart, F.; Blasé, X.; Carroll, D. L.; Czerw, R.; Foley, B.; Grobert, N.; Kamalakaran, R.; Redlich, P.; Rühle, M.; Seeger, T.; Terrones, H. *Appl. Phys. A: Mater. Sci. Process* **2002**, *74*, 355.
(10) Trasobares, S.; Stéphan, O.; Colliex, C.; Hsu, W. K.; Kroto, H. W.; Walton, D. R. M. *J. Chem. Phys.* **2002**, *116*, 8966.
(11) Sen, R.; Satishkumar, B. C.; Govindaraj, S.; Harikumar, K. R.; Renganathan, M. K.; Rao, C. N. R. *J. Mater. Chem.* **1997**, *12*, 2335.
(12) Sen, R.; Satishkumar, B. C.; Govindaraj, A.; Harikumar, K. R.; Raina, G.; Zhang, J. P.; Cheetham, A. K.; Rao, C. N. R. *Chem. Phys. Lett.* **1998**, *287*, 671.
(13) Nath, M.; Satishkumar, B. C.; Govindaraj, A.; Vinod, C. P.; Rao, C. N. R. *Chem. Phys. Lett.* **2000**, *322*, 333.
(14) Grobert, N.; Terrones, M.; Trasobares, S.; Kordatos, K.; Terrones, H.; Olivares, J.; Zhang, J. P.; Redlich, P.; Hsu, W. K.; Reeves, C. L.; Wallis, D. J.; Zhu, Y. Q.; Hare, J. P.; Pidduck, A. J.; Kroto, H. W.; Walton, D. R. M. *Appl. Phys. A: Mater. Sci. Process* **2000**, *70*, 175.
(15) Han, W. Q.; Redlich, P. K.; Seeger, T.; Emst, F.; Rühle, M.; Grobert, N.; Hsu, W. K.; Chang, B. H.; Zhu, Y. Q.; Kroto, H. W.; Walton, D. R. M.; Terrones, M.; Terrones, H. *Appl. Phys. Lett.* **2000**, *77*, 1807.
(16) Lee, C. J.; Lyu, S. C.; Kim, H. W.; Lee, J. H.; Cho, K. I. *Chem. Phys. Lett.* **2002**, *359*, 115.
(17) Tang, C.; Bando, Y.; Golberg, D.; Xu, F. *Carbon* **2004**, *42*, 2625.
(18) Glerup, M.; Castignolles, M.; Holzinger, M.; Hug, G.; Loiseau, A.; Bernier, P. *Chem. Commun.* **2003**, *20*, 2542.
(19) Liu, J.; Czerw, R.; Webster, S.; Carroll, D. L.; Park, J. H.; Park, Y. W.; Terrones, M. *Mater. Res. Soc. Symp. Proc.* **2003**, *772*, 105.
(20) Liu, J.; Czerw, R.; Carroll, D. L. *J. Mater. Res.* **2005**, *20*, 538.
(21) Andrews, R.; Jacques, D.; Rao, A. M.; Derbyshire, F.; Qian, D.; Fan, X.; Dickey, E. C.; Chen, J. *Chem. Phys. Lett*. **1999**, *303*, 467.
(22) Scofiled, J. H. *J. Electron Spectrosc.* **1976**, *8*, 129.
(23) Zhang, Y.; Gu. H.; Iijima, S. *Appl. Phys. Lett.* **1998**, *73*, 3827.
(24) Hernandez, E.; Goze, C.; Bernier, P.; Rubio, A. *Appl. Phys. A: Mater. Sci. Process* **1999**, *68*, 287.
(25) Shimoyama, I.; Wu, G. H.; Sekiguchi, T.; Baba, Y. *Phys. Rev. B* **2000**, *62*, R6053.
(26) Casanovas, J.; Ricart, J. M.; Rubio, J.; Illas, F.; Jimenez-Mateos, J. M. *J. Am. Chem. Soc.* **1996**, *118*, 8071.
(27) Tuinstra, F.; Koenig, J. L. *J. Chem. Phys.* **1970**, *53*, 1126.
(28) Lee, Y. T.; Kim, N. S.; Bae, S. Y.; Park, J.; Yu, S. C.; Ryu, H.; Lee, H. J. *J. Phys. Chem. B* **2003**, *107*, 12958.